Mon. Not. R. Astron. Soc. **000**, 000–000 (0000) Printed 10 December 2006 (MN LATEX style file v2.2)

Low frequency waves in asymmetric magnetized relativistic pair plasma

M. Gedalin[1], E. Gruman[1], and D.B. Melrose[2]
[1]*Ben-Gurion University, Beer-Sheva 84105, Israel*
[2]*Research Centre for Theoretical Astrophysics, School of Physics, University of Sydney, NSW 2006, Australia*

10 December 2006

ABSTRACT
The properties of waves in a pulsar magnetosphere are considered in the most general case of a nonneutral, current carrying, pair plasma with arbitrary distribution functions for electrons and positrons. General dispersion relations are derived for a strong but finite magnetic field, including gyrotropic terms due to the deviations from quasineutrality and the relative streaming of electrons and positrons. It is shown how the ellipticity of the wave polarization depends on the plasma parameters and angle of propagation. Two examples of plasma distributions are analyzed numerically: a waterbag distribution and a piecewise distribution that models the numerical result for pair cascades. Possible application to the interpretation of the observed circular polarization of some pulsars is discussed.

Key words: Pulsars – pair plasms – waves – low frequencies – radio emission

1 INTRODUCTION

The pulsed nonthermal radio emission of pulsars is believed to be generated in the relativistic pair plasma filling the polar cap regions of the pulsar magnetosphere (e.g. Manchester & Taylor (Manchester and Taylor1977)). This plasma is produced via electromagnetic cascade (Arons (Arons1983) and references therein) in a superstrong magnetic field. In most models (Melrose1993) the density of the pair plasma N_p exceeds by several orders of magnitude the Goldreich-Julian density $N_{GJ} = \mathbf{B}\cdot\mathbf{\Omega}/2\pi ec$ (where $\mathbf{B}$ is the pulsar magnetic field and $\mathbf{\Omega}$ is the pulsar angular velocity), although the multiplicity factor $M = N_p/N_{GJ} \gg 1$ is poorly known (Shibata et al.1998). The primary plasma (which is the source of the denser secondary plasma) is of density $\sim N_{GJ}$ and flows along the field lines with the Lorentz-factor $\gamma_{pr} \sim 10^7$. The parameters for the secondary plasma are poorly constrained. An estimate considered plausible is a flow Lorentz-factor $\gamma_p \sim \gamma_{pr}/M$ (Arons1983; Melrose1993; Shibata et al.1998) with a spread $\langle\gamma\rangle \sim \gamma_p$ in the rest frame of the plasma.

The necessity to screen out the corotational electric field (Manchester and Taylor1977) requires that the pair plasma have a nonzero charge density $N_+ - N_- = N_{GJ}$. The primary beam (Ruderman & Sutherland1975) carries a current, and current conservation requires that this current be carried outwards through the secondary plasma (Lyutikov1998). On the other hand, the condition $N_+ - N_- = N_{GJ}$ also requires a backward flowing current (Lyubarskii1992).

The properties of the waves in the pair plasma in the emission region and above it along the ray path are thought to play a significant role in influencing some features of the observed radio emission (e.g., Melrose (Melrose1995) and references therein). In particular, the pair plasma is thought to produce the outgoing radio waves (in the10^8–10^{10} Hz frequency range) through some form of plasma instability. Cyclotron (Lominadze et al.1983), curvature (e.g., Lyutikov (Lyutikov et al.1999) and references therein), and beam (Lominadze et al.1979; Usov1987; Lyubarskii1992) instabilities have been proposed. The particle energy is then either transformed directly into radio waves which are capable of escaping from the pulsar magnetosphere, or into waves that cannot themselves escape but which produce the escaping radio waves through some additional, probably nonlinear mechanism (Melrose1993; Melrose1995). In any case the features of the waves in the pair plasma are of crucial importance for understanding the radio emission mechanism.

Waves in a pair plasmas with identical distributions of electrons and positrons have been studied extensively (Lominadze et al.1979; Gedalin and Machabeli1982; Volokitin et al.1985; Arons & Barnard1986; Lyubarskii1995; Gedalin et al.1998; Melrose et al.1999; Han et al.2000) in the cold as well as in the hot regimes. For identical distributions of electrons and positrons the wave polarization is strictly linear. When the distributions are not identical the wave modes have a non-zero circular component that is of interest in the interpretation of the observed polarization. The radio emission is well known to be typically highly linearly polarized, and it is now well established that many pulsars also have a substantial circular polarization (Han et al.1998; Manchester et al.1998; von Hoensbroech et al.1998; von Hoensbroech and Lesch1999; Han et al.2000). Various suggestions for the cause of circular polar-

ization have been proposed. Specific suggestions use wave mode coupling due to the rotation (Radhakrishnan & Rankin1990; Lyubarskii & Petrova1999), refer to specific characteristics of the emission mechanism (Gil and Snakowski1990a; Gil and Snakowski1990b; Radhakrishnan & Rankin1990; Gangadhara1997; Lyutikov et al.1999), consider propagation effects (Petrova & Lyubarskii2000) or invoke nonlinear interactions (Lyutikov1999). Cheng & Ruderman (Cheng and Ruderman1977) and later Arons & Barnard (Arons & Barnard1986) suggested that the polarization may be associated with the properties of the natural wave modes in the plasma. The ellipticity of the waves in a pair plasma is nonzero if the plasma is nonneutral or if it carries a current along the magnetic field. Wave properties in a current carrying, relativistic pair plasma have been considered by Lyutikov (Lyutikov1998) for the special case where the plasma is neutral in its rest frame with a relativistic thermal (Jüttner) distribution.

In the present paper we study the effects on the wave properties of nonzero charge and current densities in a strongly magnetized, highly relativistic pair plasma with arbitrary distribution functions for the electrons and positrons. We do not assume that the charge density vanishes in either the pulsar frame or in the plasma rest frames. (Zero charge density and nonzero current density in one frame imply nonzero charge and current densities in the other frame.) We show that these conditions imply that waves with phase speed close to the speed of light speed can be substantially elliptically polarized. We study the dependence of the elliptical polarization on the plasma parameters. We illustrate the analysis with two numerical examples of different distributions. One is a waterbag distribution: it has been shown (Gedalin et al.1998; Melrose et al.1999) that this provides a semi-quantitatively correct description of the wave features apart of their damping rates. The other distribution that we choose is a piecewise continuous model for the distributions found in pair cascade calculations (Daugherty & Harding1982).

In section 2 we describe the plasma conditions from the point of view of the pulsar and plasma rest frames. The general dielectric tensor and dispersion relation are given in section 3. The wave features are summarizes in Section 4 in the infinite magnetic field limit. The generalization to a finite magnetic field, including wave polarization, is considered in section 5. The dielectric tensor is evaluated for the waterbag distribution in section 6. In section 7 we present results for the distribution that simulates the results of pair cascade calculations (Daugherty & Harding1982). We discuss the results in section 9.

2 PULSAR CONDITIONS

The plasma which fills the pulsar magnetosphere is produced in a electromagnetic cascade beginning most probably with (primary) charge particle acceleration along the magnetic field lines in the polar gap up to very high energies $\gamma_{pr} \sim 10^7$. While moving along the curved magnetic field lines the primary particles emit high energy curvature photons that, in turn, produce electron-positron plasma pairs. Alternatively the high-energy photons may be produced by Compton scattering of thermal photons from the polar cap surface (Zhang & Harding2000). This copious pair production develops in an explosive way and a relativistic dense plasma is produced in a narrow layer known as the pair production front (Arons1983), behind which a dense secondary plasma is formed. It had been thought that this dense secondary plasma would screen out the parallel electric field, but serious doubts have been raised as to whether this is possible (Shibata et al.1998).

The secondary plasma parameters depend on the details of the polar gap structure, in particular, on the electric field, the height of acceleration region and the geometry of the magnetic field (which affects both the generation of the curvature photons and also the details of the secondary pair production (Arons1983)). The density of primary particles just below the pair production front is assumed to be $N_{pr} \sim N_{GJ}$. The secondary plasma density is written as $N_p \sim MN_{GJ}$, where the multiplicity factor $M \sim 10^2 - 10^5$ is poorly determined (Shibata et al.1998; Lyutikov1998). For the sake of discussion we assume $\gamma_p \sim \gamma_{pr}/M$ for the Lorentz-factor of the secondary plasma *bulk flow* in the pulsar frame.

In what follows we use the following notation: all variables measured in the pulsar frame are primed, and non-primed variables refer to the *plasma* rest frame (not necessarily the zero-bulk-flow frame) moving with the Lorentz-factor γ_p. We use the spatial component of the 4-velocity $\mathbf{u} = \gamma\mathbf{v}/c$ (the definition is valid in both frames), so that, for motion strictly along the magnetic field lines, the transformation rules are

$$u' = \gamma_p u + u_p \gamma, \qquad \gamma' = \gamma_p \gamma + u_p u, \tag{1}$$

$$u = \gamma_p u' - u_p \gamma', \qquad \gamma = \gamma_p \gamma' - u_p u', \tag{2}$$

where $\gamma = \sqrt{1+u^2}$ (respectively, for the primed and p-subscripted variables). The invariance of the distribution function implies $f'(u') = f(u)$.

The production mechanism for the secondary pair plasma implies a distribution function in the pulsar frame that is limited by some $u'_{\min} \gtrsim 1$ from below and by some $u'_{\max}$ from above. The 4-speed $u'_{\max}$ is thought to be about an order of magnitude greater than the average $\langle u' \rangle$, where it is assumed that the distribution decreases rapidly with energy and that u_p is high. The corresponding limits in the plasma frame $u_{\min}$ and $u_{\max}$ depend on γ_p, namely, $u_{\max}$ increases with increasing Lorentz factor of the flow. This is illustrated by Figure 1 where the distribution function $f(u) = \text{const}\gamma^{-3/2}$, $|u| < u_{\max}$ is transformed from the plasma rest frame into the pulsar frame. For $u_{\max} = -u_{\min} = 1$ and $u_p = 20$ the distribution in the pulsar frame is limited by $u'_{\min} \approx 8$ and $u'_{\max} \approx 48$. For $u_{\max} = -u_{\min} = 1$ and $u_p = 2000$ the limits are $u'_{\min} \approx 800$ and $u'_{\max} \approx 4800$, while choosing $u_{\max} = -u_{\min} = 10$ with the same $u_p = 2000$ one gets $u'_{\min} \approx 100$ and $u'_{\max} \approx 40000$. For large multiplicities $M \sim 10^4 - 10^5$ one has $u_p \sim 10^2$ so that in the plasma frame $u_{\max} \sim 1 - 10$.

For a pulsar with the period of $P = 0.2\,\text{s}$ and magnetic field on the pole $B = 10^{12}\,\text{G}$ (Lyutikov1998), the Goldreich-Julian density at the pulsar surface in the polar region is $N_{GJ} \approx 3.5 \times 10^{11}\,\text{cm}^{-3}$. If the multiplicity $M \sim 10^5$ (the densest case considered), the plasma density in the pulsar frame is $N' = MN_{GJ} = 3.5 \times 10^{16}\,\text{cm}^{-3}$. For $\gamma_p \sim 10^7 M^{-1} \sim 10^2$ the plasma density in the plasma rest frame is $N \approx N'/\gamma_p \approx 3.5 \times 10^{14}\,\text{cm}^{-3}$, which gives the plasma rest frame plasma frequency of about $\omega_p = \sqrt{4\pi Ne^2/m} \approx \times 10^{12}\,\text{s}^{-1}$. Thus, the ratio (see below) $(\omega_p/\Omega)^2 \approx 10^{-14}(R/R_P)^3$ (plasma rest frame), where $\Omega = eB/mc$ is the gyrofrequency, R is the radius, and R_P is the pulsar radius. At the light cylinder, $R = R_L = cP/2\pi \approx 10^3 R_P$, the ratio $(\omega_p/\Omega)^2 \sim 10^{-5}$. For lower multiplicities the plasma density in the plasma frame $N \propto M/\gamma_p \propto M^2$ may be by 2-5 orders of magnitude lower.

The deviations from quasineutrality in the pulsar frame imply $\rho'/N'e \sim 1/M$ (Manchester and Taylor1977). The current density is also determined by the same parameter $j'/N'ec \sim 1/M$ (Lyubarskii1992; Lyutikov1998). The charge density and current

density in the plasma rest frame may be obtained from the following transformation rules:

$$\rho' = \gamma_p\rho + u_p j/c, \qquad j'/c = \gamma_p j/c + u_p\rho, \tag{3}$$

$$\rho = \gamma_p\rho' - u_p j'/c, \qquad j/c = \gamma_p j'/c - u_p\rho', \tag{4}$$

and depend strongly on the details of the density and current distribution. For example, if $j'/c = \rho' v_p/c = \rho' u_p/\gamma_p$ (all current is due to the convection of the two plasma species with different densities), in the plasma frame $\rho = \rho'/\gamma_p$, and $j = 0$. More generally, for $j'/\rho' v_p = \alpha$, one has

$$\rho = [\gamma_p(1-\alpha) + \alpha/\gamma_p]\rho', \tag{5}$$

$$j/c = (\alpha - 1)u_p\rho'. \tag{6}$$

The Lyutikov's (Lyutikov1998) assumption that $\rho = 0$ corresponds to $j'/c = \gamma_p\rho'/u_p$ or $\alpha = c^2/v_p^2$. It also means that the current in the plasma frame $j = j'/\gamma_p$ is weak. It is not clear what might ensure the fine tuning $j'/c = \gamma_p\rho'/u_p$ throughout the pulsar magnetosphere. In general, if α is not close to unity, the ratio the density and current in the plasma frame $\rho/Ne \sim j/Nec \sim \gamma_p^2/M$ and can well be large.

3 DISPERSION RELATION AND WAVE PROPERTIES

The dispersion relation is obtained from the matrix equation

$$\begin{pmatrix} n_\parallel^2 - \epsilon_{xx} & -\epsilon_{xy} & -n_\parallel n_\perp - \epsilon_{xz} \\ -\epsilon_{yx} & n^2 - \epsilon_{yy} & -\epsilon_{yz} \\ -n_\parallel n_\perp - \epsilon_{zx} & -\epsilon_{zy} & n_\perp^2 - \epsilon_{zz} \end{pmatrix} \begin{pmatrix} E_x \\ E_y \\ E_z \end{pmatrix} = 0, \tag{7}$$

where $n = kc/\omega$ is the refraction index, $n_\parallel = n\cos\theta$, $n_\perp = n\sin\theta$, θ is the angle between $\mathbf{k}$ and $\mathbf{B}_0$, and $\mathbf{B}_0 = (0, 0, B_0)$ and $\mathbf{k} = (k_\perp, 0, k_\parallel)$ are the external magnetic field and wave vector, respectively. The dielectric tensor ϵ_{ij} is determined by the plasma distribution function. The methods of calculation of the dielectric tensor are well-known and can be found elsewhere (e.g., Gedalin et al. (Gedalin et al.1998)). For our present purposes we use the expressions derived by (Gedalin et al.1998) for the case of one-dimensional distribution function $f = f(u_z)\delta(u_\perp)/u_\perp$ (cf. also Lyutikov (Lyutikov1998), Melrose el al. (Melrose et al.1999)):

$$\epsilon_{xx} = \epsilon_{yy} \equiv \epsilon_\perp = 1 + \sum_s \frac{\omega_{ps}^2}{\Omega_s^2}[\langle\gamma\rangle_s - 2n_\parallel\langle u_z\rangle_s + n_\parallel^2\langle u_z^2\gamma^{-1}\rangle_s], \tag{8}$$

$$\epsilon_{zz} \equiv \epsilon_\parallel = 1 - \sum_s \frac{\omega_{ps}^2}{\omega^2} W_s(n_\parallel) + \sum_s \frac{\omega_{ps}^2 n_\perp^2}{\Omega_s^2}\langle u_z^2\gamma^{-1}\rangle_s, \tag{9}$$

$$\epsilon_{xy} = -\epsilon_{yx} = -i\sum_s \frac{\omega_{ps}^2}{\omega\Omega_s}(1 - n_\parallel\langle u_z\gamma^{-1}\rangle_s), \tag{10}$$

$$\epsilon_{yz} = -\epsilon_{zy} = -i\sum_s \frac{\omega_{ps}^2 n_\perp}{\omega\Omega_s}\langle u_z\gamma^{-1}\rangle, \tag{11}$$

$$\epsilon_{xz} = \epsilon_{zx} \equiv Q = \sum_s \frac{\omega_{ps}^2 n_\perp}{\Omega_s^2}(\langle u_z\rangle_s - n_\parallel\langle u_z^2\gamma^{-1}\rangle_s). \tag{12}$$

(The corresponding expressions of Gedalin et al. (Gedalin et al.1998) lost γ^{-1} in ϵ_{yz}.) Here $u_z = v_z/\gamma c$, $\gamma = \sqrt{1+u_z^2}$, and averaging is defined as follows:

$$\langle\ldots\rangle = \int(\ldots)f_0(u_z)du_z, \tag{13}$$

where $f_0(u_z)$ is the equilibrium (unperturbed) distribution. The subscript s denotes summation over the plasma species (electrons and positrons). Other parameters are defined as usual: the gyrofrequency $\Omega_s = q_s B_0/m_s c$, and the plasma frequency $\omega_{ps}^2 = 4\pi N_s q_s^2/m_s$. Expressions (8)–(12) take into account both a nonzero charge density and a nonzero current density. The function W_s is defined by the integral

$$W_s(n_\parallel) = -\frac{1}{n_\parallel}\int \frac{1}{1 - n_\parallel v_z + i\tau}\frac{df_{0s}}{du_z}du_z, \tag{14}$$

with $\tau \to 0$.

The off-diagonal terms vanish identically when the distribution functions of the electrons and positrons are the same, $f_+ = f_-$. We introduce the following notation:

$$N_+ = N_0(1+\eta), \qquad N_- = N_0(1-\eta), \tag{15}$$

$$m_1 = \sum_s (1+s\eta)\langle\gamma\rangle_s, \tag{16}$$

$$m_2 = \sum_s (1+s\eta)\langle u_z\rangle_s, \tag{17}$$

$$m_3 = \sum_s (1+s\eta)\langle u_z^2\gamma^{-1}\rangle, \tag{18}$$

$$W = \sum_s (1+s\eta)W_s, \tag{19}$$

$$\delta_1 = \sum_s (1+s\eta) = 2\eta, \tag{20}$$

$$\delta_2 = \sum_s s(1+s\eta)\langle u_z\gamma^{-2}\rangle, \tag{21}$$

where $s = \pm 1$. Then the dielectric tensor takes the following form:

$$\epsilon_\perp = 1 + \Delta m_1 - 2\Delta m_2 n\cos\theta + \Delta m_3 n^2\cos^2\theta, \tag{22}$$

$$\epsilon_\parallel = 1 + \Delta m_3 n^2\sin^2\theta - Z^{-2}W, \tag{23}$$

$$\epsilon_{xy} = i\sqrt{\Delta}(\delta_2 n\cos\theta - \delta_1)Z^{-1}, \tag{24}$$

$$\epsilon_{xz} = \Delta m_2 n\sin\theta - \Delta m_3 n^2\sin\theta\cos\theta, \tag{25}$$

$$\epsilon_{yz} = -i\sqrt{\Delta}\delta_2 n\sin\theta Z^{-1}, \tag{26}$$

where $\Delta = \omega_p^2/\Omega^2$, $\omega_p^2 = 4\pi N_0 e^2/m$, $Z = \omega/\omega_p$, $\delta_1 = \rho/N_0 e$ and $\delta_2 = j/N_0 ec$. These equations are equally valid in the pulsar and plasma frames, provided that the corresponding distribution functions are used for the average calculations. In the *zero-bulk-mass-flow* frame one has $m_2 = 0$. However, it is not always convenient to work is this frame, so for the time being we leave $m_2 \neq 0$, in general.

4 INFINITE MAGNETIC FIELD LIMIT

We start our analysis of the wave features with the infinite magnetic field limit where $\Delta = 0$. There are two branches (e.g., Gedalin et al. (Gedalin et al.1998)): the electromagnetic t branch with the dispersion relation $n^2 = 1$, and the mixed LA (Langmuir-Alfven) branch with the dispersion relation

$$\frac{\omega^2}{\omega_p^2} = \frac{(n_\parallel^2 - 1)W}{n^2 - 1}. \tag{27}$$

One has $W(n_\parallel) > 0$ for $n_\parallel < 1$, so that there is only one wave in this range, namely the superluminal L-mode with $n^2 < 1$. We are particularly interested in the oblique wave with $|n^2 - 1| \ll 1$. If $n_\parallel \ll 1$ one has $W = \langle\gamma^{-3}\rangle \equiv 1/\gamma^*$. We can use this expression for W in the whole range $n_\parallel < 1$ bearing in mind (the

relatively weak) dependence of γ^* on $n_\parallel$. For the L-mode one has $\omega^2=\omega_p^2/\gamma^*$ at $n=0$, and $n^2=1-\omega_p^2\sin^2\theta/\omega^2\gamma^*$ in the high frequency limit, except for $\theta\approx 0$.

If the distributions are compact, that is, if there exists u_m such that $F=0$ for $|u_z|>u_m$, then the A-wave is undamped in the range $1<n_\parallel^2<1/v_m^2$, where $v_m^2=u_m^2/(1+u_m^2)$. We do not analyze the infinite magnetic field further here and refer the reader to earlier studies (Lominadze et al.1979; Gedalin and Machabeli1982; Volokitin et al.1985; Arons & Barnard1986; Lyubarskii1995; Gedalin et al.1998; Melrose et al.1999; Petrova & Lyubarskii2000). Here we only mention that all modes are linearly polarized (either $E_y\neq 0$ for the t-branch, of $E_x\neq 0$ and $E_z\neq 0$ for the LA-branch) in the infinite magnetic field limit.

5 FINITE MAGNETIC FIELD

If the magnetic field is not infinite, the complete dispersion equation does not split into two separate equations, and all three components of the electric field are, in general, present in the wave. The dispersion relation may be written in the form

$$A_2Z^4+A_1Z^2+A_0=0, \tag{28}$$

where

$$A_2=d_{22}(d_{11}d_{33}-d_{13}^2), \tag{29}$$

$$A_1=d_{11}d_{22}W-d_{11}d_{23}^2-d_{33}d_{12}^2+2d_{12}d_{23}d_{13}, \tag{30}$$

$$A_0=-Wd_{12}^2, \tag{31}$$

$$d_{11}=n^2\cos^2\theta(1-\Delta m_3)+2n\cos\theta\Delta m_2-(1+\Delta m_1), \tag{32}$$

$$d_{22}=n^2(1-\Delta m_3\cos^2\theta)+2n\cos\theta\Delta m_2-(1+\Delta m_1), \tag{33}$$

$$d_{13}=-n^2\sin\theta\cos\theta(1-\Delta m_3)-n\sin\theta\Delta m_2, \tag{34}$$

$$d_{12}=\sqrt{\Delta}(n\cos\theta\delta_2-\delta_1), \tag{35}$$

$$d_{23}=\sqrt{\Delta}n\sin\theta\delta_2, \tag{36}$$

$$d_{33}=n^2\sin^2\theta(1-\Delta m_3)-1. \tag{37}$$

The polarization ratios are given by

$$r_x\equiv\frac{E_x}{|\mathbf{E}|}=(d_{12}d_{23}-Z^2d_{22}d_{13})/D, \tag{38}$$

$$r_y\equiv\frac{iE_y}{|\mathbf{E}|}=Z(d_{11}d_{23}-d_{12}d_{13})/D, \tag{39}$$

$$r_z\equiv\frac{E_z}{|\mathbf{E}|}=(Z^2d_{11}d_{22}-d_{12}^2)/D, \tag{40}$$

$$D=[(d_{12}d_{23}-Z^2d_{22}d_{13})^2 + Z^2(d_{11}d_{23}-d_{12}d_{13})^2+(Z^2d_{11}d_{22}-d_{12}^2)^2]^{1/2}. \tag{41}$$

Nonzero r_y implies nonzero elliptical polarization. For an almost electromagnetic (transverse) wave $r_y\approx\sqrt{2}\approx 0.7$ would mean nearly circular polarization. Since $d_{11}d_{23}-d_{12}d_{13}\propto\sqrt{\Delta}\delta\ll 1$, the only way to have substantial elliptical polarization is to require $d_{22}\approx 0$, that is, $|n^2-1|\ll 1$, which, in turn, is possible only for $Z\gg 1$.

Let us consider the dispersion relation (28) in more detail in the pulsar frame. We are interested in the waves which do not damp on the Cerenkov resonance. In the case of an exponentially decreasing distribution, such as a relativistic thermal (Jüttner) distribution, it is sufficient to require that $n_\parallel\langle v_z\rangle<1$ (Lyutikov1998) to satisfy the weak cyclotron damping condition. However, for the power law spectrum (Daugherty & Harding1982) or flat distribution (Arons & Barnard1986) one has to require that either $n_\parallel v_{\max}<1$ or $n_\parallel v_{\min}>1$ (Gedalin et al.1998). The low-frequency longwavelength limit (far below the cyclotron resonance) the condition is stricter: $\gamma|1-n\cos\theta v|\ll\Omega/\omega$. If the polarization forms at $R\sim 10^3R_P$ (Cheng and Ruderman1977) then $\Omega\sim 10^{10}-10^{11}\,\mathrm{s}^{-1}$, while the observed radiofrequencies are in the range $10^9-10^{11}\,\mathrm{s}^{-1}$, so that $\omega/\Omega\lesssim 1$. Together with the previous condition, this gives either $-1/\gamma_{\max}\ll n_\parallel-1\lesssim 1/2\gamma_{\max}^2$ or $1/2\gamma_{\min}^2\lesssim n_\parallel-1\ll 1/2\gamma_{\max}$. For $\gamma_{\min}=\gamma_1\approx 10$ and $\gamma_{\max}=\gamma_4\approx 10^3$ the second condition cannot be satisfied. We, therefore, restrict ourselves with the range $-1/\gamma_{\max}\lesssim n_\parallel-1\lesssim 1/2\gamma_{\max}^2$.

From the previous analysis it is clear that we are interested in the range $\theta\ll 1$ and $n\approx 1$. Let us define $n_\parallel=1+\chi$, where $|\chi|\ll 1$. Expanding and retaining leading terms in small parameters χ, θ, and Δ, one finds $d_{11}=2(\chi-\chi_1)$, $d_{22}=-d_{11}d_{33}+d_{13}^2=\chi-\chi_2$, where $\chi_1=\Delta(m_1+m_3-2m_2)/2$, $\chi_2=\chi_1-\theta^2/2$. Let us first consider the case of the symmetric plasma $d_{12}=0$, $d_{23}=0$. Then the dispersion relation (28) splits into two separate dispersion relations:

$$\chi=\chi_2, \tag{42}$$

$$Z^2=\frac{W(\chi-\chi_1)}{\chi-\chi_2}. \tag{43}$$

The second dispersion relation describes the L mode (asymptotically approaching $\chi=\chi_2$) and the A mode, whose frequency is limited from above (cf. Gedalin et al. (Gedalin et al.1998)) in view of the requirement $\chi\lesssim 1/2\gamma_{\max}^2$. The A-mode is not of interest for us and is not mentioned further.

For the L mode in the high frequency range one has from (43)

$$\chi=\chi_2-\frac{W\theta^2}{Z^2}. \tag{44}$$

Since $W\lesssim\langle\gamma\rangle$ the difference between $n_\parallel$ for t (see (42)) and L modes is small at high frequencies and small angles.

Let us now analyze the complete dispersion relation (28). To leading order in small quantities it can be written as

$$4Z^2(Z^2-W)(\chi-\chi_2)^2+2\theta^2W(\chi-\chi_2)-(Z^2-W)\Delta(\delta_2-\delta_1)^2=0. \tag{45}$$

The solutions are

$$\chi-\chi_2=\frac{-\theta^2WZ^2\pm\sqrt{\theta^4W^2Z^4+4(Z^2-W)Z^2\Delta(\delta_2-\delta_1)^2}}{4Z^2(Z^2-W)}. \tag{46}$$

The refraction index $n=n_\parallel/\cos\theta=1+\chi+\theta^2/2$ in the same approximation. Eq. (46) can be used in (38)–(39) to obtain

$$\left|\frac{E_y}{E_x}\right|=\frac{2Z^2|\chi-\chi_2|}{\sqrt{\Delta}Z|\delta_2-\delta_1|}. \tag{47}$$

The relations (46) and (47) provide the general solution for the wave properties, albeit in implicit form due to W being a function of $n_\parallel$. Unfortunately, there is no universal approximation for W in the range $-1/2\gamma_{\max}<\chi<1/2\gamma_{\max}^2$, so that these relations are of limited usefulness. On the other hand, (28) together can be considered as a parametric representation of $\omega/\omega_p=Z(n)$ and $kc/\omega_p=nZ(n)$. Then (38)–(40) give the polarization features in the parametric form. In the next two sections we illustrate the use of this parametric representation with two different distributions considered in the plasma (waterbag distribution (Arons & Barnard1986)) and pulsar (power-law distribution (Daugherty & Harding1982)) rest frames. The equation (28) is solved with respect to Z, and W

is calculated analytically (for the waterbag distribution) or determined numerically (for the power-law distribution).

6 EXAMPLE 1: WATERBAG DISTRIBUTION IN THE PLASMA FRAME

In this section we consider the waterbag distribution in the plasma frame. Such distribution was first proposed as an approximation by Arons & Barnard (Arons & Barnard1986) and roughly corresponds to their described pair distribution transformed into the plasma frame. To take into account the nonzero charge and current densities, we consider the waterbag distributions for electrons and positrons that are shifted one relative to the other:

$$f_+ = \frac{1+\eta}{u_1+u_2}\Theta(u_2-u_z)\Theta(u_1+u_z), \tag{48}$$

$$f_- = \frac{1-\eta}{u_1+u_2}\Theta(u_2+u_z)\Theta(u_1-u_z). \tag{49}$$

These shifted waterbag distributions allow exact calculation of the dispersion relation in the form of algebraic equation, which greatly simplifies the analysis. We expect that the analysis will describe properly the features of the modes in the asymmetric relativistic pair plasma. Gedalin et al. (Gedalin et al.1998) have shown that more realistic distribution functions add dissipation of the waves with the phase velocities $\omega/k_\parallel < u_-$, prohibiting propagation of waves with too low phase velocities (too large $n > n_m$, where n_m is determined by the distribution function, $n_m = 1/v_m$ for the compact distribution). At the same time in the high phase velocity range, with $n < n_m$, the wave features do not depend significantly on the exact form of the distribution and usage of the waterbag distribution is justified and instructive.

With these waterbag distributions one finds:

$$m_1 = \left[u_1\gamma_1 + u_2\gamma_2 + \ln((\gamma_1+u_1)(\gamma_2+u_2))\right]\left[u_1+u_2\right]^{-1}, \tag{50}$$

$$m_2 = \eta(u_2-u_1), \tag{51}$$

$$m_3 = \left[\frac{u_1\gamma_1+u_2\gamma_2}{2} - \tfrac{1}{2}\ln\left(\frac{\gamma_1+u_1}{\gamma_2-u_2}\right)\right]\left[u_1+u_2\right]^{-1}, \tag{52}$$

$$\delta_1 = 2\eta, \tag{53}$$

$$\delta_2 = 2(\gamma_2-\gamma_1)/(u_1+u_2), \tag{54}$$

$$W = \frac{2}{u_1+u_2}\left(\frac{v_1}{1-n^2\cos^2\theta v_1^2} + \frac{v_2}{1-n^2\cos^2\theta v_2^2}\right) + \frac{\eta n\cos\theta(v_2^2-v_1^2)}{(u_1+u_2)(1-n^2\cos^2\theta v_1^2)(1-n^2\cos^2\theta v_2^2)}. \tag{55}$$

The expressions (53)–(55) are used below for the graphical presentation of the polarization. Being particularly interested in the circular (elliptical) polarization, we use the ratio $r_y = iE_y/\sqrt{E_x^2+E_y^2+E_z^2}$ as the signature of ellipticity (E_x and E_z are in phase and are chosen to be real, so that iE_y is also real).

Figure 2 shows the ellipticity as a function of frequency for several different angles of propagation: $\theta = 1^\circ$, 2°, and 5°. Only one mode is shown for clarity. The plasma parameters chosen are: $\Delta = 10^{-8}$, $u_0 = 2$, $\bar{u} = 0.01$, $\eta = 0.005$, which corresponds to $\delta_1 = 0.01$ and $\delta_2 = 0.009$. The ellipticity r_y rapidly decreases to nearly zero as the propagation angle increases. At small angles the ellipticity is still not negligible, despite the very small parameter Δ. The ellipticity increases with increasing frequency. It should be noted that only the range $\omega/\omega_p \ll \sqrt{1/\Delta}$ is of physical significance because of the initial assumption $|\omega - k_z v_z| \ll \Omega\langle\gamma\rangle$. That means that only the range $\omega/\omega_p < 10^3$ should be seriously considered.

Figure 3 shows the same dependence but for $\Delta = 10^{-6}$. The ellipticity is substantially stronger even at the frequency $\omega/\omega_p \sim 10^2$.

Figure 4 shows the dependence of the effect on the sign of η and $\bar{u}$: $\eta = 0.005$, $\bar{u} = 0.01$ (crosses), $\eta = 0.005$, $\bar{u} = -0.01$ (diamonds), $\eta = -0.005$, $\bar{u} = 0.01$ (triangles), $\eta = -0.005$, $\bar{u} = -0.01$ (circles). For this figure $\Delta = 10^{-6}$ and $\theta = 1^\circ$. Note that the sense of the polarization depends on the sign of the parameters.

The sense of the polarization depends also on the magnitude of the parameters, as can be seen from Figure 5, where we show the ellipticity for two different values of the parameter η and $\bar{u}$: $\eta = 0.005$, $\bar{u} = 0.01$ (crosses), $\eta = 0.01$, $\bar{u} = 0.01$ (diamonds), and $\eta = 0.005$, $\bar{u} = 0.02$ (triangles). In general, sense of polarization is determined by the sign of $d_{11}d_{22} - d_{12}^2$ (see Eq. (39)) which depends on the refraction index or frequency. For $|n^2-1| \ll \sin^2\theta \ll 1$, the sense of the polarization is determined by $\delta_2 - \delta_1$, that is, by the gyrotropic term ϵ_{12}.

7 EXAMPLE 1: POWER-LAW DISTRIBUTION IN THE PULSAR FRAME

Working in the plasma rest frame has the advantage of the direct comparison with the conventional results of the plasma physics, usually derived in the center-of-mass frame. However, all analytically and numerically determined pair distributions are obtained in the pulsar frame. Moreover, consideration in the pulsar frame allows direct comparison with observations without additional frame transformation. In this section we analyze the distribution of the kind:

$$f = \begin{cases} 0, & u < u_1 \\ f_m(\gamma/\gamma_2)^{\alpha_1}, & u_1 < u < u_2 \\ f_m(\gamma/\gamma_2)^{\alpha_2}, & u_2 < u < u_3 \\ f_m(\gamma_3/\gamma_2)^{\alpha_2}(\gamma/\gamma_3)^{\alpha_3}, & u_3 < u < u_4 \\ 0, & u_4 < u \end{cases}. \tag{56}$$

A distribution of this shape was obtained by Daugherty & Harding (Daugherty & Harding1982). The parameters derived from their Fig. 7 are as follows (very approximately): $u_1 = 10$, $u_2 = 30$, $u_3 = 300$, and $u_4 = 3000$, while the multiplicity $M \sim 10^4$. These parameters are found for the Crab pulsar. For pulsars with periods around 0.5 s the multiplicity is $\sim 10^3$. The energies are also expected to be lower. The power spectra indices are $\alpha_1 \approx 2$, $\alpha_2 \approx -3/2$, and $\alpha_3 \approx -2$. The analytic fit for this distribution (smoothed by properly chosen $\tanh$s) and its counterpart in the frame moving with the velocity u_2 is shown in Figure 6. We choose such distribution for both the positrons and electrons, normalizing them in the ratio $1+\eta$ to $1-\eta$, and with a relative drift $\bar{u} = u_+ - u_-$ applied to all $u_{1,2,3,4}$. Figure 7 shows these distributions for the case where $\eta = 10^{-4}$ and $\bar{u} = -5$, so that in the pulsar frame the relative density and current are $\delta_1 = 2\times10^{-4}$ and $\delta_2 = 10^{-4}$, respectively. It is worth noting that the frame moving with the velocity u_2 is not the zero-bulk-flow frame, which has $u_p = 44.5$.

The angle $\theta = 5^\circ$ in the plasma frame corresponds to the angle $\approx \theta/2\gamma_p \approx 0.1^\circ$ in the pulsar frame. Figure 8 shows the dependence of the frequency of L mode on $n_\parallel - 1$ for different angles of propagation: circles stand for $\theta = 0.3^\circ$, diamonds for $\theta = 0.1^\circ$,

triangles for $\theta = 0.03^\circ$, and crosses for $\theta = 0.001^\circ$. The parameter $\Delta = 10^{-5}$. The corresponding ellipticity is shown in Figure 9. The ellipticity for $\theta = 0.3^\circ$ is negligible and is not shown. The ellipticity increases with increasing frequency and decreasing angle. For $\theta = 0.001^\circ$ the mode is completely circularly polarized at $\omega/\omega_p > 40$. The transition from complete linear polarization to the circular polarization is rather sharp. For larger angles of propagation the elliptic polarization corresponds in fact to the transition region from the linear to circular polarization, only this region is rather wide.

8 CIRCULAR POLARIZATION IN PULSAR RADIO EMISSION

Data on circular polarization (CP) of pulsar radio emission has been reviewed by (Han et al.1998; Han et al.2000). In brief, (Han et al.2000) reported that: (1) CP can occur in both core and conal emission, (2) it can reverse sense (handedness), not necessarily in the centre of the profile, (3) there is no correlation with the position angle (PA) of the linear polarization for core emission, (4) there is a strong correlation for conal emission between the sense of circular polarization and the sign of the time derivation of PA (right hand CP and increasing PA), and (5) there is no systematic variation of CP with frequency, and many pulsars exhibit similar CP over a wide range of frequencies. These data refer to the CP averaged over many individual pulsars. In some pulsars the CP in individual pulsars is high and varies from pulse to pulse, such that the pulse-averaged CP is very much smaller than the characteristic CP in an individual pulse (Manchester et al.1975; Stinebring et al.1984). There is no entirely satisfactory explanation for the origin CP (Radhakrishnan & Rankin1990; Kazbegi et al.1991; Radhakrishnan1992). The possible explanations can be separated into two classes: the CP is intrinsic to the emission process, or the CP is imposed as a propagation effect. The very high degree of CP in some individual pulses is difficult to reconcile with any possible pulsar emission mechanism, and we concentrate here on the possibilities of explaining the CP in terms of a propagation effect. There are several possibilities, most of which rely in some way on an electron-positron asymmetry.

We discuss one possibility: the emission occurs in a region where the modes are essentially linearly polarized, with the emission mechanism favouring one mode over the other. There is evidence that the radiation does escape as a mixture of two orthogonal wave modes, with opposite CPs, and that the net polarization depends on the ratio of the intensities in these two modes (McKinnon & Stinebring2000). As the radiation propagates outward it should stay in its initial wave modes, as the properties of these modes, including the ellipticity of the polarization, change as the plasma parameters and the angle of propagation change. Our results show that the ellipticity depends strongly on the parameter ω_p/Ω, in the sense that the CP is not significant when this parameter is too small. For example, for the power-law distribution in the pulsar frame (extending from $u_{\rm min} = 1$ to $u_{\rm max} = 300$, with the multiplicity $M \sim 10^4$ and density and current parameters $\delta_1 = 2 \times 10^{-4}$ and $\delta_2 = 10^{-4}$, respectively), elliptical polarization is significant only for $\theta \lesssim 0.1^\circ$ in the pulsar frame. This range may be considered as the transition zone from the linear polarization regime (at larger angles) to the circular polarization regime. CP dominates at angles $\sim 0.01^\circ$. This model implies that the natural modes are linear in the inner magnetosphere and elliptical only far from the surface at the distance of about 10^3 pulsar radii (depending on the plasma and magnetic field characteristics). If the radio spectrum forms well inside the magnetosphere, at $R \lesssim 10^2 R_p$ (Cordes1992), the electromagnetic waves propagate outward initially as linearly polarized waves, evolving into (partly) circularly polarized waves as ω/ω_p, ω_p/Ω, θ change. At some point, called the polarization limiting region, the birefringence of the plasma becomes unimportant and the polarization is fixed at that point.

The polarization limiting region (Cheng and Ruderman1977; Petrova & Lyubarskii2000), is where the characteristic distance over which waves in the two modes get out of phase becomes larger than the dimensions of the system. Specifically, it is where the difference between the refractive indices for the two (nearly degenerate almost electromagnetic) modes satisfies $|n_1 - n_2| \lesssim \lambda/L$, where λ is the wavelength and L is the typical scale of the plasma/magnetic field inhomogeneity (curvature). This condition implies the breakdown of the so-called adiabatic walking (Cheng and Ruderman1977), where the local polarization is determined by the properties of the local modes in the approximation of the geometrical optics. In order that significant CP be observed, the natural modes must be significantly elliptically polarized at the polarization limiting region (Cheng and Ruderman1977). The location of the polarization limiting region depends on the propagation angle, the frequency, and on the inhomogeneous of the plasma (Arons & Barnard1986; Petrova & Lyubarskii2000). A detailed investigation is warranted, but has yet to be carried out.

As mentioned there are several other ways in which CP can arise as a propagation effect. One way is through cyclotron damping: cyclotron damping can affect the polarization by preferentially damping one mode compared with the other as the waves propagate through the region where the cyclotron resonance occurs (Kennett et al.2000). Cyclotron damping is different for the two CPs whenever the distributions of electrons and positrons are not identical. Another possibility is that the radiation is scattered by inhomogeneities along the ray path, and such scattering leads to CP that depends on the ellipticity of the natural modes in the scattering region, as well as on the details of the scattering. A systematic investigation of these and other possible causes for the CP is needed, and any such investigation will require a knowledge of the CP of the natural modes and of its dependence on the plasma parameters.

9 CONCLUSIONS

We derive a general dispersion relation for low-frequency, $|\omega - k_\parallel v_\parallel| \ll \Omega/\gamma$, waves in a relativistic pair plasma with nonzero charge and current densities in the plasma, and with distributions of electrons and positrons in either the pulsar or plasma frames. The inclusion of nonzero charge and current densities implies that the natural wave modes are elliptically polarized. The ellipticity depends on the charge and current densities, denoted here by the parameters ρ/Ne and j/Nec, and also depends on both the wave frequency and angle of propagation. A motivation for this investigation is the interpretation of the circular polarization (CP) of pulsar radio emission. Although the interpretation of the CP remains unclear, a plausible explanation is that the radiation emerges in a mixture of the two natural wave modes, and that these are elliptically polarized due to the nonneutrality of the plasma. The results derived in this paper are needed for any systematic investigation of the interpretation of the CP as a propagation effect.

ACKNOWLEDGMENTS

The authors are grateful to Yu. Lyubarsky for stimulating discussions and to Qinghuan Luo for helpful comment. This research was supported in part by Israel Science Foundation under grant No. 170/00-1.

REFERENCES

Arons J., 1983, ApJ., 266, 175.
Arons J. & Barnard J.J., 1986, ApJ, 302, 120.
Cheng A.F. & Ruderman M.A., 1977, ApJ, 212, 800.
Cordes J.M., in *The Magnetospheric Structure and Emission Mechanisms of Radio Pulsars* (eds T.H. Hankins, J.M. Rankin and J.A. Gill, Pedagogical University Press, Zielona Góra, Poland, 1992), p. 253.
Daugherty J.K. & Harding A.K., 1982, ApJ, 252, 337.
Gangadhara R.T., 1997, A&A, 327, 155.
Gedalin M.E. & Machabeli G.Z., 1982, Soviet Astron. Lett., 8, 153.
Gedalin M., Melrose D.B. & Gruman E., 1998, Phys. Rev. E, 57, 3399.
Gil J.A. & Snakowski J.K., 1990a, A&A, 234, 237.
Gil J.A. & Snakowski J.K., 1990b, A&A, 234, 269.
Han J.L., Manchester R.N., Xu R.X. & Qiao G.J., 1998, MNRAS, 300, 373.
Han J.L., Manchester R.N. & Qiao G.J., 2000, in Kramer, M., Wex, N. & Wielebinski, R. (eds) 2000, Pulsar Astronomy – 2000 and Beyond, Proc. IAU Colloquium 177, Astron. Soc. Pacific., p. 251.
von Hoensbroech A. & Lesch H., 1999, A&A, 342, L57.
von Hoensbroech A., Kijak J. & Krawczyk A., 1998a, A&A, 334, 571.
Kazbegi A.Z., Machabeli G.Z. & Melikidze G.I., 1991, MNRAS, 253, 377.
Kennett, M.P., Melrose, D.B. & Luo, Q., 2000, J. Plasma Phys. (in press).
Lominadze J.G., Mikhailovskii A.B. & Sagdeev R.Z., 1979, Zh. Eksp. Teor. Fiz., 77, 1951.
Lominadze J.G., Machabeli G.Z. & Usov V.V., 1983, ApSS, 90, 19.
Lyubarskii Y.E., 1992, A&A, 265, L33.
Lyubarskii Yu.E., 1995, Astrophys. Space Phys. Rev., 9, 1.
Lyubarskii Y.E. & Petrova S.A., 1999, ApSS, 262, 379.
Lyutikov M., 1998, MNRAS, 293, 447.
Lyutikov M., 1999, ApJ, L37, 525.
Lyutikov M., Machabeli G. & Blandford R., 1999, ApJ, 512, 804.
Manchester R.N., Han J.L. & Qiao G.J., 1998, MNRAS, 295, 280.
Manchester R.N. & Taylor J.H. , Pulsars, 1977, Freeman, San Fransisco.
Manchester, R.N., Taylor, J.H. & Huguenin, G.R., 1975, ApJ, 196, 83.
McKinnon, M.M. & Stinebring, D.R., 2000, ApJ, 529,435.
Melrose D.B., in Pulsars as Physics Laboratories, (eds R.D. Blandford, A. Hewish, A.G. Lyne and L. Mestel, Oxford University Press, 1993) p. 105.
Melrose D.B., 1995, J. Astrophys. Astron., 16, 137.
Melrose D.B., Gedalin M., Kennett M.P. & Fletcher C.S., 1999, J. Plasma Phys., 62, 233.
Petrova S.A. & Lyubarskii Y.E., 2000, A&A, 355, 1168.
Radhakrishnan, V. 1992, in T.H. Hankins, J.M. Rankin & J.A. Gil (eds), The magnetospheric structure and emission mechanisms of radio pulsars, proceedings of IAU 128, Pedagogical University Press, Zielona Góra, p. 367.
Radhakrishnan V. & Rankin J.M., 1990, ApJ, 352, 822.
Ruderman M.A. & Sutherland P.G., 1975, ApJ, 196, 51.
Shibata S., Miyazaki J. & Takahara F., 1998, MNRAS, 295, L53.
Stinebring, D.R., Cordes, J.M., Weisberg, J.M., Rankin, J.M., & Boriakoff, V., 1985, ApJS, 55, 247 & 279.
Usov V.V., 1987, ApJ, 320, 333.
Volokitin A.S., Krasnoselskikh V.V. & Machabeli G.Z., 1985, Sov. J. Plasma Phys., 11, 531.
Zhang B. & Harding A.K., 2000, ApJ, 532, 1150.

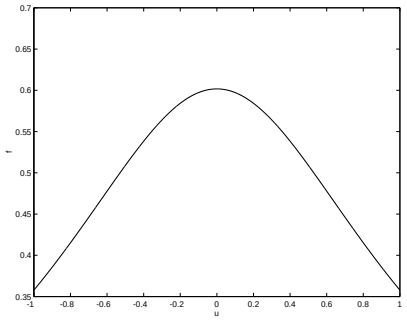

(a)

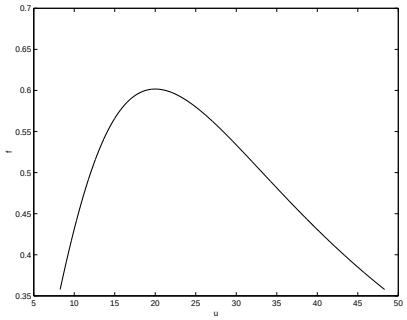

(b)

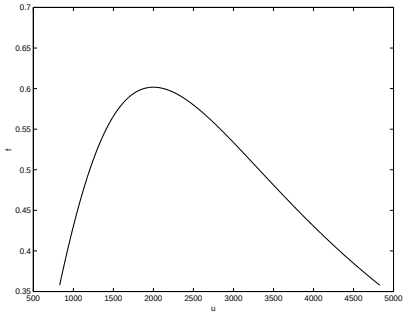

(c)

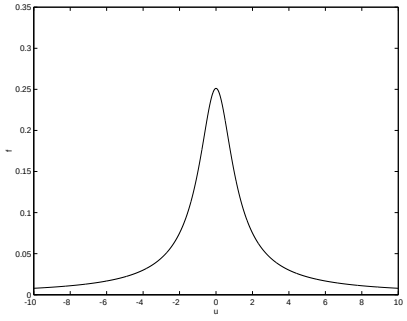

(d)

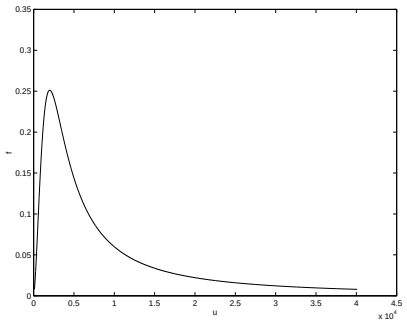

(e)

Figure 1. Transformation of the distribution $f(u) \propto \gamma^{-3/2}$ from the plasma ((a) and (c)) to the pulsar ((b), (c), and (e)) rest frame. The parameters are chosen as follows: for (a) and (b) $u_{\max} = -u_{\min} = 1$, $u_p = 20$; for (c) $u_{\max} = -u_{\min} = 1$, $u_p = 2000$; for (d) and (e) $u_{\max} = -u_{\min} = 10$, $u_p = 2000$.

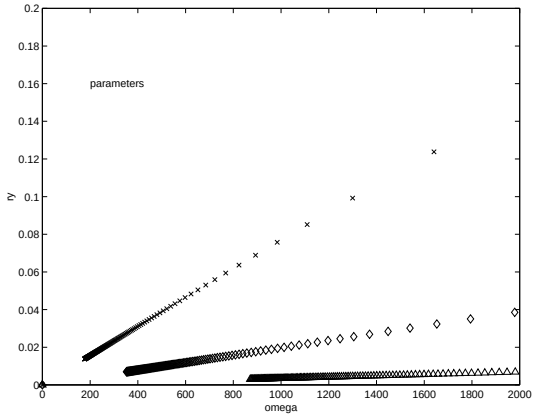

Figure 2. Ellipticity for $\Delta = 10^{-8}$, $u_0 = 2$, $\bar{u} = 0.01$, $\eta = 0.005$, and different propagation angles $\theta = 1^\circ$ (crosses), $\theta = 2^\circ$ (diamonds), and $\theta = 5^\circ$ (triangles), as a function of frequency.

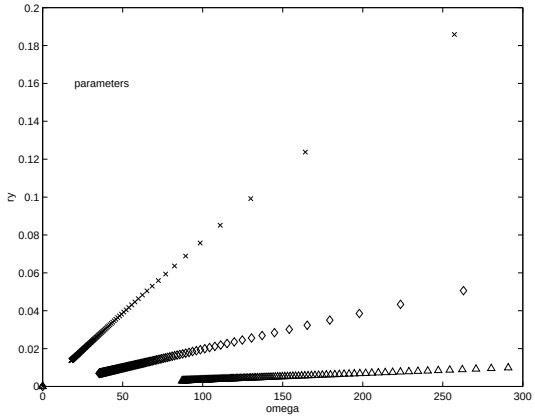

Figure 3. Ellipticity for $\Delta = 10^{-6}$, $u_0 = 2$, $\bar{u} = 0.01$, $\eta = 0.005$, and different propagation angles $\theta = 1^\circ$ (crosses), $\theta = 2^\circ$ (diamonds), and $\theta = 5^\circ$ (triangles), as a function of frequency.

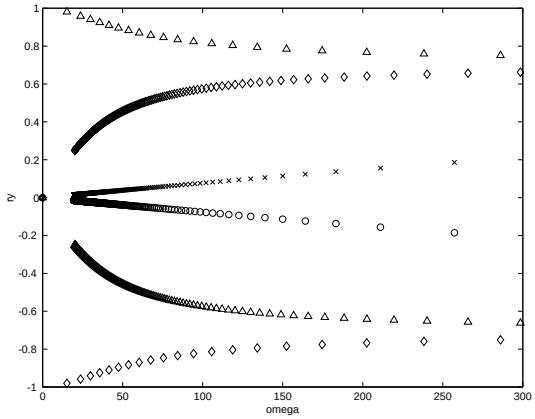

Figure 4. Ellipticity for $\Delta = 10^{-6}$, $\theta = 1^\circ$, and various pairs of η and $\bar{u}$: $\eta = 0.005$, $\bar{u} = 0.01$ (crosses), $\eta = 0.005$, $\bar{u} = -0.01$ (diamonds), $\eta = -0.005$, $\bar{u} = 0.01$ (triangles), $\eta = -0.005$, $\bar{u} = -0.01$ (circles).

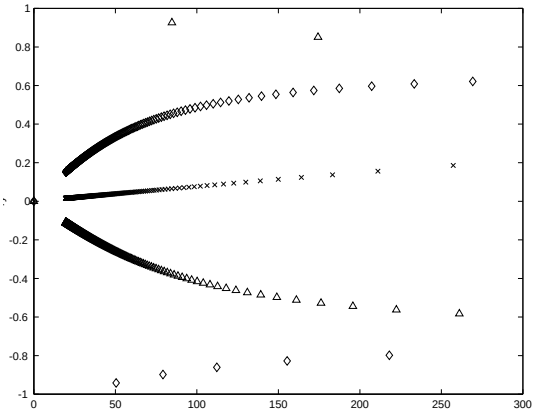

Figure 5. Ellipticity for $\Delta = 10^{-6}$, $\theta = 1^{\circ}$, and two the following values of η and $\bar{u}$: $\eta = 0.005$, $\bar{u} = 0.01$ (crosses), $\eta = 0.01$, $\bar{u} = 0.01$ (diamonds), and $\eta = 0.005$, $\bar{u} = 0.02$ (triangles).

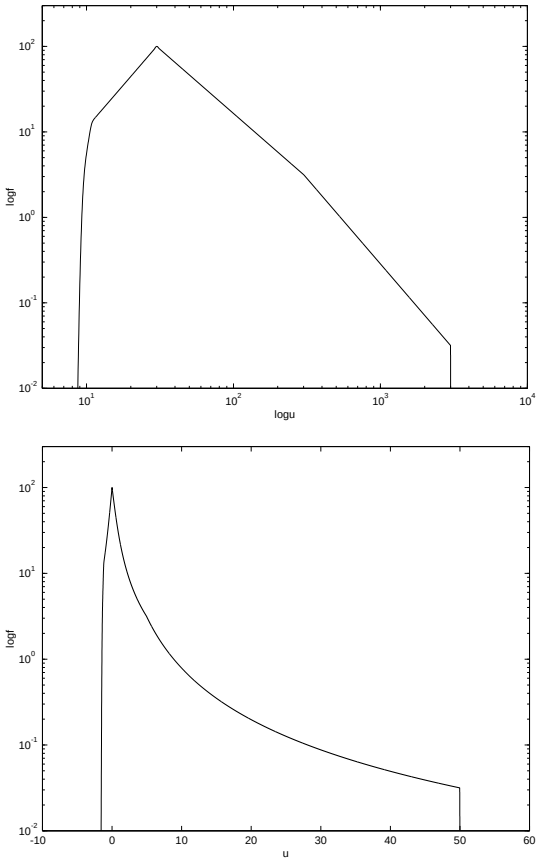

Figure 6. (a) The distribution numerically found by Daugherty & Harding (Daugherty & Harding1982) in the pulsar frame. (b) The same distribution transformed in the frame moving with the velocity of the distribution maximum. Not normalized.

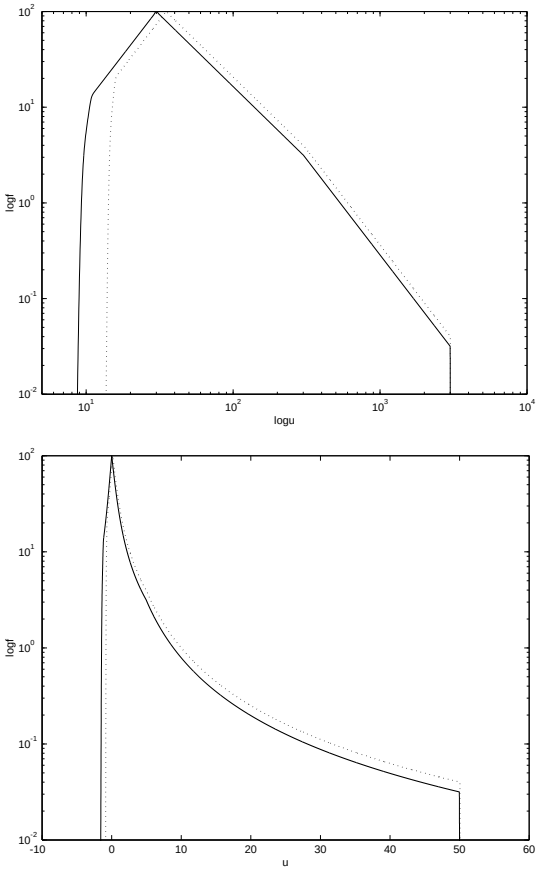

Figure 7. The two shifted distributions in the pulsar (a) and positron (b) frame. See explanations in the text.

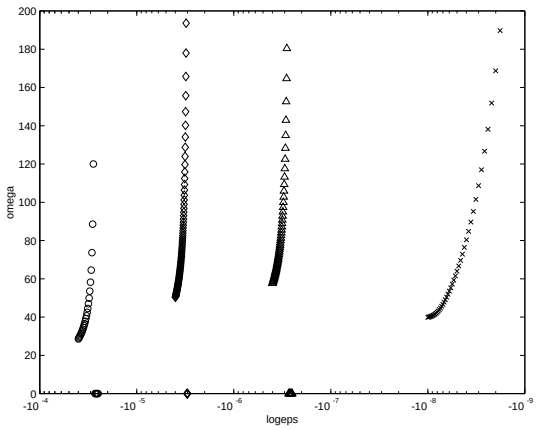

Figure 8. Frequency vs. $n_{\|} - 1$ for $\Delta = 10^{-5}$ and various angle of propagation: $\theta = 0.3^{\circ}$ (circles), $\theta = 0.1^{\circ}$ (diamonds), $\theta = 0.03^{\circ}$ (triangles), and $\theta = 0.001^{\circ}$ (crosses).

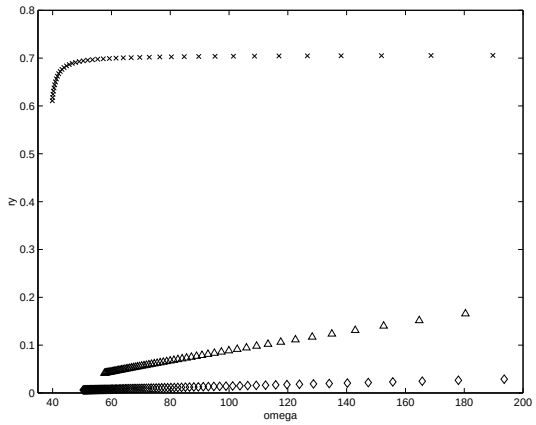

Figure 9. Ellipticity vs. frequency for $\Delta = 10^{-5}$ and various angle of propagation: $\theta = 0.1^\circ$ (diamonds), $\theta = 0.03^\circ$ (triangles), and $\theta = 0.001^\circ$ (crosses).